Article:
Radosavljevic, A, Radovanovic, J, Milanovic, V et al. (1 more author) (2015) Cubic GaN/AlGaN based quantum wells optimized for applications to tunable mid-infrared photodetectors. Optical and Quantum Electronics, 47 (4). 865 - 872. ISSN 0306-8919

https://doi.org/10.1007/s11082-014-0016-y

Cubic GaN/AlGaN based quantum wells optimized for applications to tunable mid-infrared photodetectors

A. Radosavljević[1, 2], J. Radovanović[1], V. Milanović[1] and D. Indjin[3]

[1] School of Electrical Engineering, University of Belgrade, Bulevar kralja Aleksandra 73, 11120 Belgrade, Serbia
[2] Ph* group, Vinča Institute of Nuclear Sciences, University of Belgrade, P.O.B. 522, Belgrade, Serbia
[3] School of Electronic and Electrical Engineering, University of Leeds, Leeds LS2 9JT, UK
e-mail: radovanovic@etf.bg.ac.rs

Abstract We propose a method which delivers optimal cubic GaN/AlGaN quantum well (QW) profiles such that both the Stark effect and peak intersubband absorption from the ground to the first excited electronic state, in a prescribed range of bias electric fields, are maximized. Our method relies on the Genetic Algorithm which finds globally optimal structures with a predefined number of embedded layers. We investigate simple rectangular quantum wells with embedded step layers for applications in tunable mid-infrared photodetectors. The effects of band nonparabolicity are taken into account to refine our model.

Keywords Quantum well, Stark effect, Intersubband absorption, Tunable photodetectors, Genetic Algorithm

1 Introduction

Group III–nitride semiconductors and their alloys have attracted a lot of attentions in the past two decades because of their promising applications in nanostructured optoelectronic devices. Besides their application in devices operating on the basis of interband transitions (laser and light emitting diodes in blue-green and ultraviolet spectral range [1-3]), electronic and optical properties of GaN and related materials make them particularly suitable for intersubband (ISB) based devices. Due to large values of the conduction band discontinuity and very short ISB absorption recovery times measured in femtoseconds, GaN/Al(Ga)N planar nanostructures are becoming the foremost system for ISB devices operating at telecommunication wavelengths, such as fast multiple quantum well (QW) photodetectors or modulators [4-8]. On the other hand, by changing the QW thickness and Al molar fraction in AlGaN alloy it is possible to tune the ISB absorption peak wavelength to mid-infrared (mid-IR) or terahertz (THz) spectral range, as well [5,9-11].

Until recently, the hexagonal (wurtzite) nitrides, stable phase of nitrides, were mainly investigated. However, a large piezoelectric field causes a significant built-in electric field at the interfaces of thin layers composing a nanostructure. This complicates the tuning of ISB absorption central wavelength and design of photodetectors based on planar nanostructures. Thanks to the advances in material growth, nowadays it is possible to successfully grow high quality thin films of cubic (zinc blende) nitrides. These materials are characterized by the absence of such internal fields, thus being more convenient for applications in the infrared radiation detection.

Over the past few years, cubic Gan/AlGaN QW based photodetectors have been extensively investigated for detection of mid-IR and THz radiation [5,12-14]. In this work we considered the design of optimal QW profiles in external electric field for the possible applications in tunable mid-IR photodetectors.

2 Theoretical considerations

It is well-known that the shift in energy levels caused by an external electric field (the Stark effect), translates into bias dependent optical properties [15], with possible applications in optoelectronics. In this paper we investigate QW structures with the aim to design tunable detectors of mid IR radiation, based on the Stark effect. The goal is to achieve maximal tuning spectrum for a predefined range of bias electric fields. In order to keep the photodetector efficiency large, it is important to keep the absorption as high as possible while tuning the transition wavelength λ. While these two requirements can be conflicting in case of a simple symmetric rectangular QW, which has the largest transition dipole moment but shows too small a Stark effect to be of practical interest, it is possible to find satisfactory solutions by examining a multitude of possible asymmetric QWs profiles. We considered asymmetric step QWs with a predetermined number of embedded layers (potential steps) presuming that by suitably tailoring of their profile one may design the desired photodetector based on these structures. Our approach relied on finding the optimal QWs with a preset total number of layers, which meet the above preconditions, by using the Genetic algorithm (GA).

We start our calculations from the fractional absorption on the transition between two bound states, which is given by

$$A = \frac{e^2}{2\overline{n}\,\varepsilon_0 \omega m_0^2 c} \int_0^{+\infty} \left|P_{if}\right|^2 F_{if}\left(k_t^2\right) \delta\left(E_f - E_i - \mathrm{h}\omega\right) d\left(k_t^2\right), \qquad (1)$$

where m_0 is the free electron mass, e electron charge, E_f and E_i are the energies of final and initial state, $\overline{n}$ the refractive index, c the vacuum velocity of light, ε_0 is the vacuum dielectric permittivity, $\mathrm{h}\omega$ is the photon energy, k_t is the in-plane wavevector, and F_{if} denotes the difference of Fermi-Dirac functions for states i and f. In addition, P_{if} is the momentum matrix element which may be written as $P_{if} = -im_0\omega M_{if}$, where $M_{if} = \int \eta_i^* z \eta_f dz$ is the dipole matrix element and $\eta_{i,f}$ are the z-components of corresponding wavefunctions. In reality, the absorption profile given by (1) is smeared by the Lorentz broadening, and the fractional absorption may then be written as

$$A = \frac{e^2 \omega}{2\overline{n}\,\varepsilon_0 c} \left|M_{if}\right|^2 \int_0^{+\infty} L\left(k_t^2\right) F_{if}\left(k_t^2\right) d\left(k_t^2\right), \qquad (2)$$

where the dipole transition matrix element is taken to be independent of k_t, and L is the normalized Lorentzian given by

$$L = \frac{\Gamma/2\pi}{\left[\mathrm{h}\omega - \left(\Delta E_{if}(0) + \mathrm{h}^2 k_t^2 / 2m_{t_{if}}\right)\right]^2 + \left[\Gamma/2\right]^2}. \qquad (3)$$

In the above expression, $\Delta E_{if}(0)$ is the transition energy at $k_t = 0$, Γ is the homogeneous part of the transition linewidth, and $m_{t_{if}}^{-1} = m_{t_i}^{-1} - m_{t_f}^{-1}$ is the difference of reciprocal transverse electron effective masses in the initial and the final state.

Owing to the difference term F_{if} in Eq. (2), it is evident that the Fermi level should be placed between the transition states for the purpose of achieving maximal absorption. This condition is fulfilled by appropriate doping of the nanostructure with donor atoms, and the position of the Fermi level is then found numerically from the condition of global electro-neutrality [16].

The positions of bound states in planar nanostructures are found from the conventional single-band envelope-function Hamiltonian, which is a valid approximation in this case. To refine the model, we have incorporated the nonparabolicity of the conduction band through energy dependent effective mass

$$m^*(z,E) = m^*(z)\left(1 + \frac{E - U(z)}{E_g(z)}\right), \qquad (4)$$

where $m^*(z)$, $U(z)$ i $E_g(z)$ are the spatially dependent parabolic effective mass, the potential profile and the energy bandgap, while E is the bound state energy. This model predicts the bound-state energies rather accurately [17].

3 Numerical results

The material parameters used in numerical calculations are: $m_{AlN} = 0.33m_0$ [18], $m_{GaN} = 0.11m_0$ [5], $E_{gAlN} =$ 6.7eV, $E_{gGaN} = 3.45$eV [5, 18]. The GaN/AlN conduction band offset in Γ valley (minimum) was taken as $\Delta E_c = 1.6$eV [5, 7]. We used pure GaN as the well material and $Al_xGa_{1-x}N$ as the barrier and embedded layer material. Vegard's law (linear interpolation) was used for the alloy layers. Since cubic AlN is an indirect band gap material, there is a crossover between direct and indirect band gap in AlGaN alloy for a certain value of Al mole fraction. Indirectness of band gap would introduce excessive line broadening, because of strong coupling of QW states with the continuum in the barriers, followed by decreased absorption peak. Since the interest of our study is to find structures which would deliver maximal absorption, we considered only the case with direct energy band gap in the barriers, thus limiting the maximal Al mole fraction to x = 0.7 and the value of barrier height to 1.12eV, as in [9]. Surface doping in QWs is kept at the level of $5\text{x}10^{12}/\text{cm}^2$ while the parameter Γ (Eq. (3)) was set to 60 meV.

It should be noted that many body corrections have an influence on the optical properties of the studied semiconductor nanostructures [19,20]. Furthermore, the results depend on the value of the dephasing of the absorption lines (Γ) used in calculations. In bulk semiconductors, as well as in semiconductor heterostructures (such as QW in electric field considered here) linewidths for all the trasitions have a complex dependence on the wavevector and frequency, as explained in detail in Refs. [21-23]. In this paper we have selected an average value of Γ, which is an assumption often used in the literature. An exact approach which relies on 'full k' approximation [21 -22] would certainly provide a more complete and precise description, along with more accurate numerical results. This will be included in our future work work in order to increase the predictive power of the calculations.

Since we sought optimal QW profiles, our GA-based optimization procedure relied on varying values of structural QW parameters within physically or technologically feasible limits in order to find maximal tuning range of central wavelengths, while keeping the peak absorption at an acceptable level. GA is a well-known stochastic method for finding the set of input parameters which provide the optimal value of a given target function. It is very convenient for the optimization of QW profiles because it approaches globally optimal step QWs, with both the Stark effect and the absorption coefficient having large values, provided that the target function has been carefully defined. For the problem considered in this work the best choice for the target function is

$$F_a = A_{\max}(K_{\max})A_{\max}(K_{\min})\left[E_{if}(K_{\max}) - E_{if}(K_{\min})\right]^2, \qquad (5)$$

which ensures that our criteria are fulfilled. Here A_{max} is the peak absorption value, and E_{if} is the corresponding transition energy [9].

In our previous research [9] the goal was to propose a method for designing cubic GaN/AlGaN planar nanostructures for the applications in the whole infrared spectral range. Hence we also predict therein which type of nanostructures (quantum well or Bragg confined superstructure) can be best used for applications in specific parts of IR spectrum. Here we focus our attention on mid-IR tunable photodetectors based on Stark effect in QWs with different number of embedded layers. Therefore we will

first briefly summarize the main findings obtained for QWs with one embedded layer obtained in [9], since we feel it is necessary for better understanding of the subsequently obtained results in this work and for drawing the overall conclusions about asymmetric QW based tunable photodetectors.

The optimal QW profile with one embedded layer (obtained with the target function (5)) has the following parameters: d = 3.84nm, s = 5.16nm, x = 0.08, and is shown in Fig.1, for maximal external electric field applied. Table 1 provides the values of subbands minima, the Fermi level, dipole matrix element, absorption, as well as the transition energy and wavelength, when minimal and maximal electric field is applied parallel to the QW layers growth direction. One can observe a decrease of the initial energy level position, along with a slight increase in the final energy level, which results in higher transition energy, i.e. in shifting of the transition wavelength towards lower values in the mid-infrared spectral range. Fig 2 shows absorption profiles for different values of applied bias electric field.

Table 1 Results obtained by the application of electric field K perpendicular to the planes of the layers. $E_{i,f}$ are the initial and the final energy state at $k_t = 0$, E_{if} is the transition energy, E_{fermi} is the Fermi level, λ is the transition wavelength, M_{if} is the dipole matrix element and A the absorption [9]

K[kV/cm]	E_i[eV]	E_f[eV]	E_{if} [eV]	E_{fermi}[eV]	λ [μm]	$\lvert M_{if}\rvert$ [nm]	A[%]
20	0.076	0.205	0.129	0.173	9.64	1.244	1.21
200	0.040	0.215	0.175	0.144	7.08	1.105	1.45

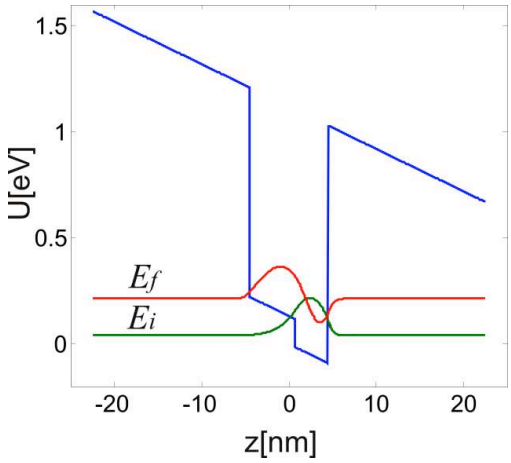

Fig. 1 Conduction band profile of the optimized asymmetric quantum well with one embedded layer, in external electric field of 200 kV/cm. The wavefunctions corresponding to the lowest two energy levels are also shown [9]

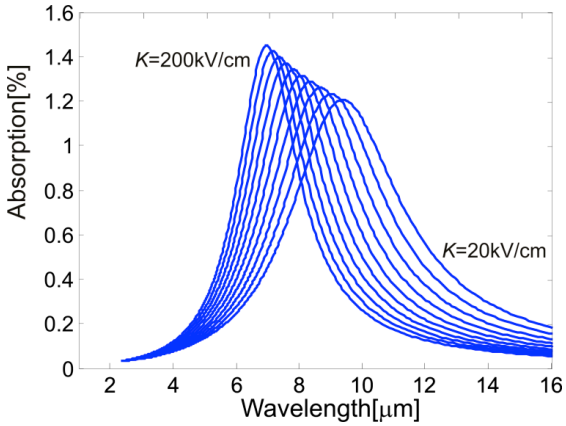

Fig. 2 The absorption profile of the optimized asymmetric quantum well with one embedded layer, subjected to external electric field. Absorption lines are plotted for different values of electric field with the increment of 20 kV/cm going from the right to the left hand side of the figure [9]

Next, we increased the number of embedded layers to two and performed the same optimization procedure. In this case there are five parameters to be varied: the width of the well d and of the two embedded layers s_1 and s_2, and the Al mole fraction x_1 and x_2 in these layers. Optimal structural parameters obtained using the same target function are: d = 9.09nm, s_1 = 0.92nm, x_1 = 0.18, s_2 = 6.1nm, x_2 = 0.08. Corresponding QW profile for maximal external field is shown in Fig.3. In Table 2 are listed the values of subbands minima, the Fermi level, dipole matrix element, absorption, as well as the transition energy and wavelength, when minimal and maximal electric field is applied parallel to the QW layers growth direction. Fig 4 depicts changes in absorption profile when external electric field is varied with an increment of 20kV/cm between minimal and maximal value.

Table 2 Results obtained by the application of electric field K perpendicular to the planes of the layers. $E_{i,f}$ are the initial and the final energy state at $k_t = 0$, E_{if} is the transition energy, E_{fermi} is the Fermi level, λ is the transition wavelength, M_{if} is the dipole matrix element and A the absorption

K[kV/cm]	E_i[eV]	E_f[eV]	E_{if} [eV]	E_{fermi}[eV]	λ [μm]	$\lvert M_{if}\rvert$ [nm]	A[%]
20	0.129	0.209	0.080	0.21	15.33	1.62	0.96
200	0.089	0.218	0.129	0.18	9.55	1.12	0.99

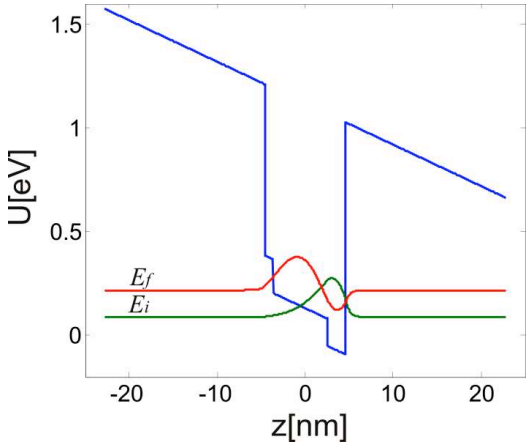

Fig. 3 Conduction band profile of the optimized asymmetric quantum well with two embedded layers, in external electric field of 200 kV/cm. The wavefunctions corresponding to the lowest two energy levels are also shown

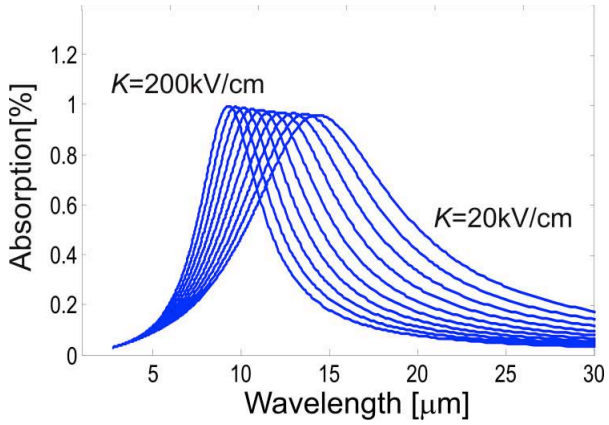

Fig. 4 The absorption profile of the optimized asymmetric quantum well with one embedded layer, subjected to external electric field. Absorption lines are plotted for different values of electric field with the increment of 20 kV/cm going from the right to the left hand side of the figure

Consequences of application of external field, such as decreasing of transition wavelength and slight increasing of absorption, are noticeable in this case, as well. Obtained wavelength tuning range of 9.55μm – 15.33μm is even larger than in the previous case (7.08μm-9.64μm). However, absorption is lower within the applied electric field range, in comparison to the case of QW with one embedded layer. Another thing to be observed is the similarity between the two profiles with one and two embedded layers (Fig. 1 and Fig. 3). The second embedded layer almost reaches the technological limit for the width of grown layers which indicates that QW profile with two layers tends to approach the profile with only one layer. Therefore, increasing the number of layers leads to better final results for wavelength tuning, but at the expense of increased complexity of QW profile, which tends to resemble the profile depicted in Fig. 1, and lower photodetector efficiency due to lower absorption. Along with increased computational time necessary to perform the optimization, this makes the structures with too many layers impractical.

4 Conclusions

In this work, we presented GA-based optimization procedure suitable for the design of tunable photodetectors comprising cubic GaN/AlGaN QWs. We observed asymmetric QWs with embedded layers in externally applied bias electric field perpendicularly to the QW layers. Optimizations were performed in order to fulfill two criteria: maximal intersubband absorption and maximal tuning range for central transition wavelengths within the specified range for values of electric field. For the case of QW with one embedded layer, it was shown that the Stark effect, caused by an external bias electric field in the range of 20kV/cm-200kV/cm can be used for the central transition wavelength tuning in the mid-IR spectral range (7.08μm-9.64μm). Further addition of embedded layers leads to a larger tuning range. However, due to increased complexity, computational time consumption and lower absorption, structures with too many layers may be unsuitable for applications.

Acknowledgment

The authors acknowledge support from MPNS COST ACTION MP1204 - TERA-MIR Radiation: Materials, Generation, Detection and Applications and BMBS COST Action BM1205 - European

Network for Skin Cancer Detection using Laser Imaging, as well as the Ministry of Education, Science and Technological Development (Republic of Serbia), project ev.no. III 45010.

References

[1] S. Mohammad and H. Morkoç, "Progress and prospects of group-III nitride semiconductors," *Progress in Quantum Electronics* **20**, 361-525, 1996.

[2] J. Schörmann, "Cubic AlGaN/GaN Structures for Device Application," Paderborn University (Dissertation), 2007.

[3] H. Morkoç, Handbook of Nitride Semiconductors and Devices, Weinheim: WILEY-VCH, Verlag GmbH & Co. KGaA, 2008.

[4] M. Beeler, E. Trichas and E. Monroy, "III-nitride semiconductors for intersubband optoelectronics: a review," *Semiconductor Science and Technology* **28**, 074022, 2013.

[5] H. Machhadani, M. Tchernycheva, S. Sakr, L. Rigutti, R. Colombelli, E. Warde, C. Mietze, D. As and F. Julien, "Intersubband absorption of cubic GaN/Al(Ga)N quantum wells in the near-infrared to terahertz spectral range," *Physical Review B* **83**, 075313 , 2011.

[6] H. Machhadani, P. Kandaswamy, S. Sakr, A. Vardi, A. Wirtmüller, L. Nevou, F. Guillot, G. Pozzovivo, M. Tchernycheva, A. Lupu, L. Vivien, P. Crozat, E. Warde, C. Bougerol, S. Schacham, G. Strasser, G. Bahir, E. Monroy and F. Julien, "GaN/AlGaN intersubband optoelectronic devices," *New Journal of Physic* **11,** 125023, 2009.

[7] E.A. DeCuir Jr, M. Manasreh, E. Tschumak, J. Schörmann, D. As and K. Lischka, "Cubic GaN/AlN multiple quantum well photodetector," *Applied Physics Letters,* **92**, 201910, 2008.

[8] E.A. DeCuir Jr, E. Fred, M. Manasreh, J. Schörmann, D. As and K. Lischka, "Near-infrared intersubband absorption in nonpolar cubic GaN/AlN," *Applied Physics Letters,* **91**, 041911, 2007.

[9] A. Radosavljević, J. Radovanović and V. Milanović, "Optimization of cubic GaN/AlGaN quantum well-based structures," *Solid State Communications* **182**, 38-42, 2014.

[10] P. Kandaswamy, H. Machhadani, C. Bougerol, S. Sakr, M. Tchernycheva, F. Julien and E. Monroy, "Midinfrared intersubband absorption in GaN/AlGaN superlattices on Si(111) templates," *Applied Physics Letters* **95**, 141911, 2009.

[11] G. Ariyawansa, M. Rinzan, M. Strassburg, N. Dietz, A. Perera, S. Matsik, A. Asghar, I. Ferguson, H. Luo and H. Liu, "GaN/AlGaN heterojunction infrared detector responding in 8–14 and 20–70μm ranges," *Applied Physics Letters* **89**, 141122, 2006.

[12] D.J. As and C. Mietze, "MBE growth and applications of cubic AlN/GaN quantum wells," *Physica Status Solidi A* **210**, 474–479, 2013.

[13] C. Mietze; E.A. DeCuir Jr, M.O.Manasreh, K. Lischka, D.J. As,"Intrasubband transitions in cubic AlN/GaN superlattices for detectors from near to far infrared," *Physica Status Solidi C* **8**, 1204-1207, 2011.

[14] D. J. As, "Recent developments on non-polar cubic group III-nitrides for," *SPIE Proceedings, Quantum Sensing and Nanophotonic Devices VII* **7608**, 76080, 2010.

[15] J. Radovanović, V. Milanović, Z. Ikonić and D. Inđin, "Quantum-well profile optimization for maximal Stark effect and application to tunable infrared photodetectors," *Journal of Applied Physics,* **91**, 525-527, 2002.

[16] J. Radovanović, V. Milanović, Z. Ikonić and D. Inđin, "Optimal design of GaN-AlGaN Bragg-confined structures for intersubband absorption in the near-infrared spectral range," *IEEE Journal of Quantum Electronics* **39**, 1297 - 1304, 1998.

[17] C. Sirtori, F. Capasso, J. Faist and S. Scandolo, "Nonparabolicity and a sum rule associated with bound-tobound and bound-to-continuum intersubband transitions in quantum wells," *Physical Review B* **50**, 8663-8674, 1994.

[18] A. Westmeyer, S. Mahajan, K. Bajaj, J. Lin, H. Jiang, D. Koleske and R. Senger, "Determination of energy-band offsets between GaN and AlN," *Journal of Applied Physics* **99**, 013705, 2006.

[19] S. Schmitt-Rink, C. Ell, H. Haug, "Many-body effects in absorption, gain and luminescence spectra of semiconductor quantum-well structures," *Physical Review B* **33**, 1183, 1986.

[20] D. S. Chemla, Jagdeep Shah, "Many-body and correlation effects in semiconductors," *Nature* **411**, 549-557, 2001.

[21] T. Schmielau, M. Pereira, "Nonequilibrium many body theory for quantum transport in terahertz quantum cascade lasers ", *Appl. Phys. Lett.* **95**, 231111, 2009.

[22] T. Schmielau, M. Pereira, "Impact of momentum dependent matrix elements on scattering effects in quantum cascade lasers", *Phys. stat. sol .(b)* **246**, 329, 2009.

[23] T. Schmielau, M. Pereira, "Momentum dependent matrix elements in quantum cascade lasers", *Microelectronics J.* **40,** 869, 2009.